F 6511

PREDICTION OF MIXING ENERGY LOSS IN A SIMULTANEOUSLY HEATED AND COOLED ROOM: PART 2—SIMULATION ANALYSES ON SEASONAL LOSS

N. Nakahara, Ph.D., P.E.
Associate Member ASHRAE

H. Ito, Ph.D.

ABSTRACT

The importance of predicting the total amount of mixing energy loss (ML) *during a heating period in a simultaneously heated and cooled room is described within the context that estimating the building energy consumption is imperative for saving energy. Regressive models for estimating the* ML *have been developed based on the experimental results described in Part 1. The* ML *can be related to the various design/control factors of the air distribution system with sufficient accuracy for practical use. Case studies for estimating the seasonal properties of heat actually supplied to a space were conducted for a typical building in a standard climate in Japan using the dynamic heat-load calculation method, which includes a regressive model of the ML. The influences of certain factors, such as operating conditions and outside wall insulation, on the seasonal heat consumption are quantitatively discussed.*

INTRODUCTION

An accurate estimate of yearly energy consumption is indispensable for enlarging the energy-saving effects of a heating, ventilating, and air-conditioning (HVAC) system. The estimation process is generally divided into three stages or calculations: the space heating and cooling loads, referred to as the "heat load"; the energy load on HVAC equipment; and the primary energy. Calculation of the heat load is the most important of the three since the other processes depend on its result. Improving the accuracy of the heat load calculation is, therefore, a very significant problem in estimating the exact building energy consumption. Air movement in a real room is much more complex, so the amount of heat actually supplied to the room might be different from the value calculated based on the assumption that supply air will completely mix with room air. Therefore, the heat load should be defined as the amount of heat to be actually supplied from the outlet to the room, and it is imperative to take into account the influence of complex room air motion. The subject of space-energy mixing loss in a simultaneously heated and cooled room is one of the phenomena that enable realization of the difference in heat load between the actual and calculated amounts. As described in Part 1, the mixing energy loss (*ML*) originates mainly from natural convection between two zones and interaction between heated air and cooled air.

This paper is based on data obtained from the experiments described in Part 1. The data were processed to fit the heat load calculation as described above.

Experiments in a simulated full-scale office room resulted in the quantification of the *ML* under various design/control factors of typical air distribution systems. The experiments were carefully designed, so the results can be taken as a universal estimation of a heat load that includes the *ML*. Therefore, this paper first proposes models for easily estimating the *ML* from various design/control factors. Models were developed by applying multiple regression analysis using more than 100 pieces of experimental data. The number of experiments (129) is believed to be sufficient to ensure reliability.

Second, this paper proposes a simulation program for evaluating the properties of heat supplied to a simultaneously heated and cooled room based on the dynamic heat-load calculation computer code that was reformed to involve the regressive model of *ML* and other functions. Case studies on the seasonal amount of heat load were conducted under various representative factors, and the seasonal properties of heat requirements were discovered.

Part of this paper was described in a Japanese version (Ito and Nakahara 1987).

FACTORS INVOLVED IN MODELS

One-hundred twenty-nine experiments were conducted to clarify the influences of various design/control factors of

Nobuo Nakahara is a professor and **Hisahiro Ito** is an assistant professor in the Department of Architecture, School of Engineering, Nagoya University, Nagoya, Japan.

air distribution systems on the *ML*. These experiments were mainly classified into four series. However, all of the results can be evaluated and analyzed on the same ground, since unified measures and procedures were adopted.

The following factors, discerned through the four series of experiments, were the dominant factors affecting the *ML*.

1. Setpoint air temperature differential between the perimeter and interior zone: This factor has the greatest influence on the *ML*. A decrease in the setpoint air temperature in the perimeter zone, compared to that of the interior zone, drastically reduced the mixing energy-loss-ratio (*MLR*), which is defined as the amount of *ML* divided by the sum of the perimeter-zone heating load and the interior-zone cooling load.
2. Discharge direction of heated air from perimeter fan-coil unit: Three levels of discharge inclination in the vertical, upward direction were examined. A 30° inclination yielded the lowest *MLR* among 0°, 30°, and 90°.
3. Perimeter depth: Reducing the perimeter depth decreases the *MLR*.
4. Temperature sensor location for the perimeter-zone fan-coil unit: Several locations were discussed for the perimeter-zone temperature sensor: the return air intake, the side of the supply outlet, the front center of the fan-coil unit, and 200 mm from the front of the fan-coil unit. This factor can have a subtle influence on the *MLR* depending on the presence of a panel heater and a storage heat load.
5. Air change rate in the interior zone: An increase in the air change rate causes a rise in the *MLR* because the potential for diffusion of the cooled air into the perimeter zone is increased.
6. Type of interior air outlet: Three types of outlets were examined: anemostat diffusers, a radial-flow outlet, and a grille. The anemostat diffusers and the radial-flow outlet were mounted on the ceiling; the grille was mounted on the high sidewall facing the outside wall. It was observed that the radial-flow outlet yields a lower *MLR* than the horizontal grille register.
7. Depth of hanging wall: The hanging wall is installed at the boundary between the perimeter zone and the interior zone. Its depth has a complicated influence on the *MLR* due to interactions with the discharged Archimedes number of heated air in the perimeter and the location of the interior temperature sensor. The discharge angle also has an indirect influence.
8. Perimeter heating load offset by the fan-coil unit: An increase in the perimeter heating load, due to heat transfer through the outside wall and heat stored in the structure, heightened the potential of the *ML* since it resulted in an increase of the heat supplied to the space. However, when a panel heater is used simultaneously with the fan-coil unit, as is the case in this study, the effects of the heating load corresponding to the fan-coil unit and that corresponding to the panel heater must be evaluated separately.
9. Interior-zone cooling load: The interior-zone cooling load heightens the productive potential of the *ML* for the same reason as for the perimeter-zone heating load.

In addition, other factors had weak but complicated influences as interactive factors affecting the *ML*: the discharge Archimedes number of the fan-coil unit, the type of air outlet of the perimeter-zone fan-coil unit, the shape/location of the perimeter-zone panel heater, the perimeter-zone heating load corresponding to the panel heater, the location of the interior-zone temperature sensor, and the type/location of the interior return air intake. All of these factors, which are illustrated in Figure 1, were used for developing regressive models.

DEVELOPMENT OF MODELS

Direct Estimation Model

A simple model, in which the MLR is directly linked to many design/control variables, was developed for the first trial. It was presupposed that the *MLR* would be linearly related to the factors and interactions, which will be referred to as variables.

$$MLR = a_o + \Sigma a_i X_i \qquad (1)$$

where X_i is the ith variable, a_i is the regressive coefficient, and a_o is the regressive constant. Only statistically significant variables are included in Equation 1.

Ventilation Model (Indirect Estimation Model)

If an estimation model can touch upon the qualitative mechanism of the objective problem, it will be much more useful for comprehension and explanation of this phenomenon. A series of experiments determined that the setpoint air temperature differential between the perimeter zone and the interior zone strongly influenced the *ML*. Therefore, for the second test, a model was developed based on the assumption that the *ML* would be dominated by heat exchange between the perimeter and interior zones through ventilation. The theory of ventilation by pressure differential through the two separate openings of the boundary plane was applied, as shown in Figure 2.

The airflow rates caused by the pressure differential between the two zones through the openings can be calculated with the following equations:

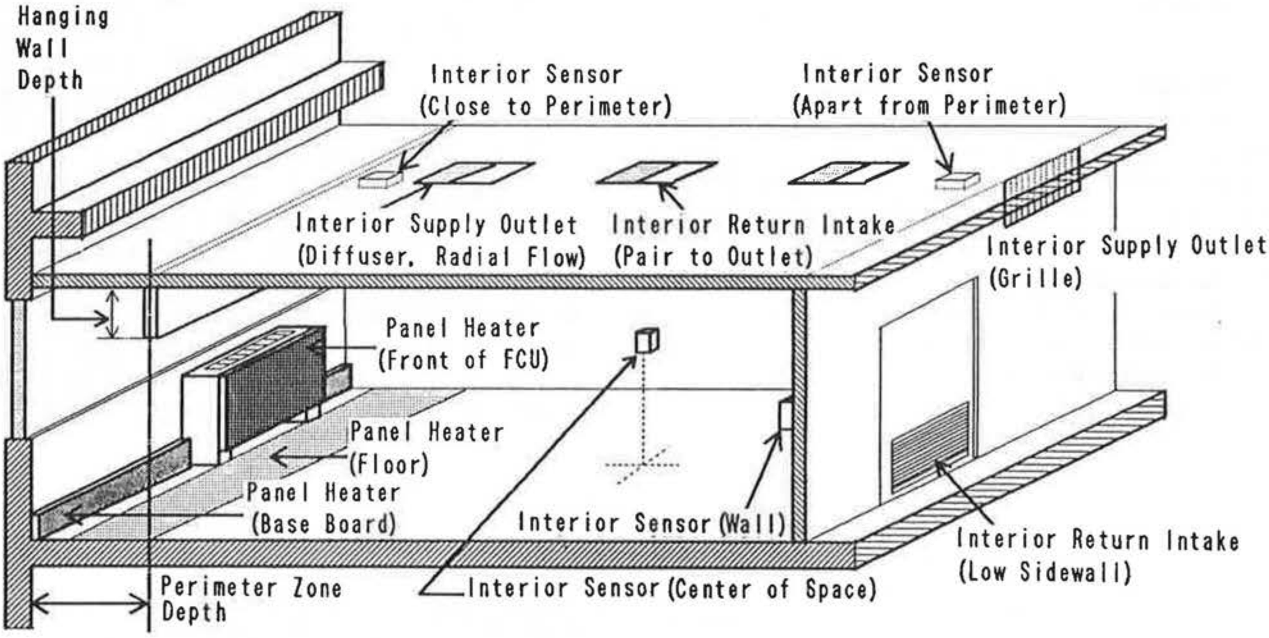

Figure 1 *Factors affecting the mixing energy loss.*

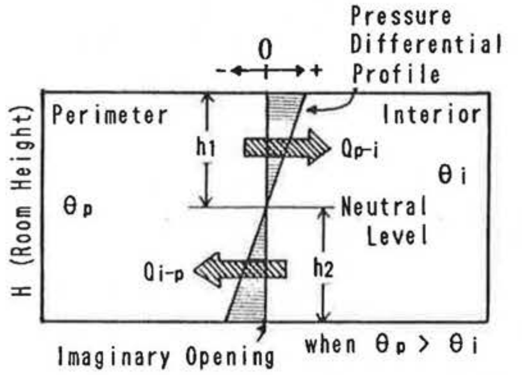

Figure 2 *Natural ventilation model: Natural ventilation generates due to the setpoint air temperature differential.*

$$Q_{p-i} = 3600\int_0^{h_1} \alpha W \sqrt{\frac{2g}{\gamma_p}|\Delta\gamma| y \, dy} \; , \qquad (2)$$

$$Q_{i-p} = 3600\int_0^{h_2} \alpha W \sqrt{\frac{2g}{\gamma_i}|\Delta\gamma| y \, dy} \; . \qquad (3)$$

To develop a simplified model, the temperature of each zone is assumed to be spatially uniform. The flow coefficient of the opening, α, is the unique parameter of the model; it is related to variables and identified in the same manner as the direct estimation model. V_{p-i} must be equal to V_{i-p} from the perspective that air volume is in equilibrium in each zone; γ_p is approximately equal to γ_i, since the temperature variations are small. The same value can therefore be deduced for both h_1 and h_2. Based on these considerations, Equations 2 and 3 can be written as one equation as follows:

$$V = V_{p-i} = V_{i-p} \qquad (4)$$

$$= 2400\,\alpha W \left(\frac{H}{2}\right)^{1.5} \sqrt{\frac{2g}{\gamma_p}\,|\,\Delta\gamma\,|}$$

$$= 2400\,\alpha W \left(\frac{H}{2}\right)^{1.5} \sqrt{\frac{2g\,\Delta\theta}{273 + \theta_p}} \; .$$

Since the *ML* can be defined as the amount of heat transfer with this airflow, it can be calculated with the following formula:

$$ML = 2c\gamma V\,|\,\Delta\theta\,| \; . \qquad (5)$$

The temperature differential in this equation, $\Delta\theta$, is fundamentally the setpoint temperature differential, but it is assumed to be affected by the supply air temperature differentials in both zones as follows:

$$\Delta\theta = t_p - t_i + \xi(\Delta t_p + \Delta t_i) \; . \qquad (6)$$

Through trial and error, ξ was given as 0.1 for the sake of establishing a high correlation in the regressive analysis, which will be discussed later. The flow coefficient, α, is assumed to be linearly related to many design/control variables as expressed by the following equation and identified by regression analysis:

$$\alpha = b_o + \Sigma\, b_i\, X_i \; . \qquad (7)$$

Verification

By applying nominal scaled factors, such as the location of the temperature sensor and the type of outlet, to the multiple regression analysis, they are represented by dummy variables of either 1 or 0. For example, when three types of factors exist, three variables are allocated for each type; the objective variable was 1 and the other two variables were 0.

The results identified for the direct estimation model and the ventilation model are shown in Table 1. By studying the standardized regression coefficient, the effects of various factors can be compared. As expected, the influence of the setpoint temperature differential between the perimeter zone and interior zone was the largest. The relationships between the measured values and the estimated values for the amount of the *ML* are shown in Figure 3 for each model. Both models have higher values for the coefficients of the correlations, and almost all of the estimated values were within the standard error range for estimations. It was, therefore, concluded that both models are sufficiently accurate and highly reliable. Furthermore, both models have many applications, as nearly all the factors that must be considered in practical design are involved. The direct estimation model was used in the simulation analysis, which will be described later, because it yields slightly higher regression coefficients than the ventilation model.

TABLE 1
Model Parameters

	Factors (X_i)		MLR		α	
			a_i	a_i^*	b_i	b_i^*
A	Set-Point Air Temperature Differential between Perimeter and Interior Zone [℃]		27.8	0.680	0.140	0.613
B	Depth of Hanging Wall [m]		16.7	0.055	7.82×10^{-2}	0.048
C	Depth of Perimeter Zone [m]		4.87	0.098	1.42×10^{-3}	0.053
D	Archimedes Number of FCU on Natural Log Scale		-2.12	-0.128	-7.10×10^{-3}	-0.081
E	Perimeter Heating Load Offset by FCU [W/m]		-8.60×10^{-3}	-0.034	-1.62×10^{-5}	-0.019
F	Perimeter Heating Load Offset by Panel Heater [W/m]		-0.129	-0.281	-7.65×10^{-4}	-0.294
G	Sensor Location for Perimeter FCU	Front Center of FCU	-16.6	-0.224	-1.00×10^{-3}	-0.003
		200mm from Front Center of FCU	-2.73	-0.010	1.41×10^{-2}	0.010
		Side of Supply Air Outlet	6.42	0.065	6.50×10^{-2}	0.123
		Return Air Intake	0.00	0.000	0.00	0.000
H	Induce Performance of Room Air in FCU Outlet	High	1.45	0.019	1.24×10^{-2}	0.030
		Low	0.00	0.000	0.00	0.000
I	Type/Location of Panel Heater	Floor	28.2	0.355	0.212	0.490
		Front of FCU	11.1	0.111	0.203	0.373
		Baseboard along Low Outside wall	6.42	0.066	0.195	0.358
		None	0.00	0.000	0.000	0.000
J	Interior Cooling Load [W/m²]		-0.263	-0.098	2.35×10^{-4}	0.016
K	Interior Air Change Rate [h^{-1}]		2.04	0.225	1.41×10^{-2}	0.296
L	Sensor Location for Interior AHU Control	Ceiling (close to Perimeter)	5.14	0.065	-1.63×10^{-2}	-0.039
		Ceiling (apart from Perimeter)	6.57	0.082	1.16×10^{-2}	0.026
		Sidewall(middle height of room)	0.00	0.000	0.00	0.000
M	Type of Interior Supply Outlet	Radial	12.2	0.152	2.20×10^{-2}	0.052
		Register Grille	18.1	0.194	0.103	0.204
		Anemostat	0.00	0.000	0.00	0.000
N	Type of Interior Return Intake	Low Sidewall	-18.5	-0.230	0.113	-0.258
		Pairs to Outlet	-1.29	-0.011	4.53×10^{-2}	-0.072
		Pairs to Outlet Excluding One Module close to Perimeter	0.00	0.000	0.000	0.000
O	Air Change Rate Differential between Perimeter and Interior Zone (P-I) [h^{-1}]		-0.341	-0.133	-5.66×10^{-4}	-0.040
	Regressive Constant		-28.9			-0.255
	Regressi[illegible] Coefficient of Correlations		0.866		0.857	

1. a_i and b_i are regressive coefficients. a_i^* and b_i^* are standarized regressive coefficients, by which the effects of variables can be estimated.
2. Nominal-scaled variables (G, H, I, L, M and N) are represented by dummy variables, either 1 or 0. For each valiable, element applied actually is replaced by 1 , and the others are replaced by 0.
3. Perimeter heating load is divided by the width of outside wall.

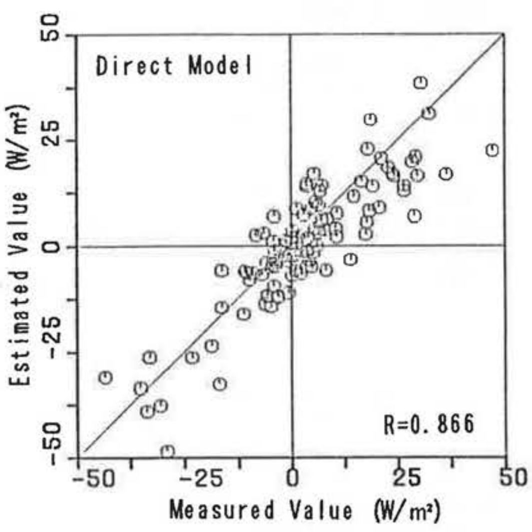

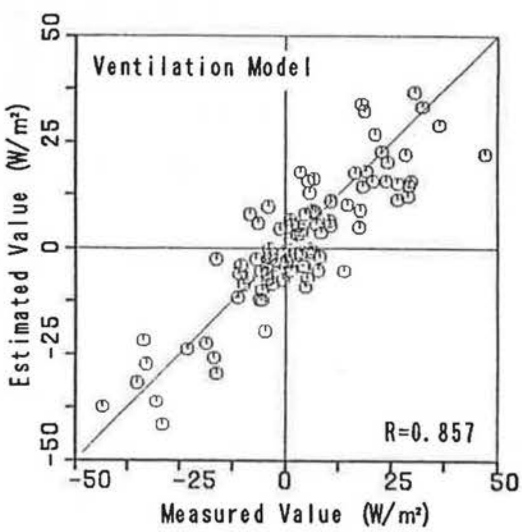

Figure 3 *Relations between the calculated values and the measured values.*

SIMULATION

Building Structure

The office plan used for the simulation study is shown in Figure 4. A center-core plan type is used, and all four outside walls are assumed to be of the same structure, so that the influence of direction on the *ML* can be evaluated impartially. The story height is 3.6 m and the ceiling height is 2.6 m. The depths of the perimeter zone and the interior zone are fixed at 3 m and 9 m, respectively, throughout all simulations.

Two types of outside wall construction were investigated, one using low insulation and the other using high insulation. Details of the wall construction are shown in Table 2. The heat conductance of opaque wall was 8.43 $W/m^2 \cdot K$ for the low-insulation wall and 0.69 $W/m^2 \cdot K$ for the high-insulation wall. Furthermore, the window surface area and the presence of a blind installed inside the window were taken into account. Since the high-insulation wall is able to reduce the perimeter heating load, it may decrease the *ML* and *MLR*.

Systems

The system using panel heaters along with fan-coil units for perimeter-zone heating was examined. The panel heater was mounted on the front surface of every fan-coil unit. The surface area of each heater was equal to that of the fan-coil unit. Ceiling-mounted anemostat diffusers or high sidewall-mounted grilles were used for interior-zone cooling. These systems are assumed to be controlled separately in each zone. Since a four-pipe fan-coil unit system was applied, no energy mixing would occur in the unit based on alternate heating and cooling. Furthermore, all apparatuses were preset to have enough capacity for the

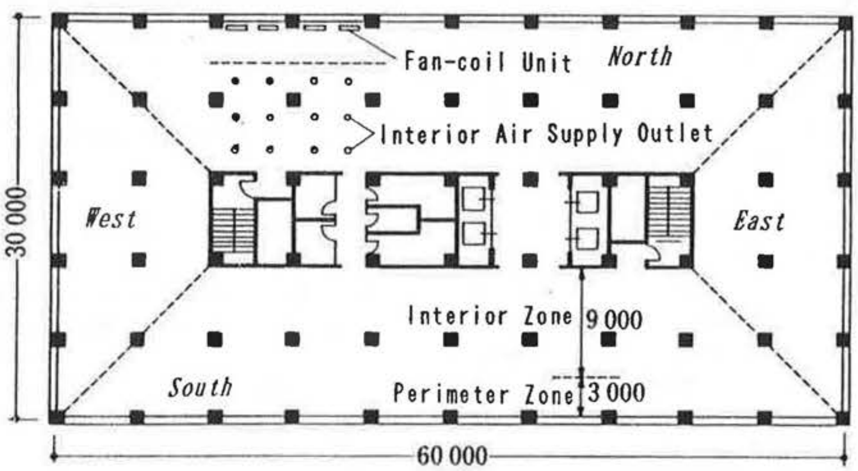

Figure 4 *Model office.*

TABLE 2
Levels of Elements Examined in Simulation Analysis

Factors	Level I	Level II
Outside Wall Inslulation	Low Insulation	High Insulation
Opaque Wall Materials	(outside) Plaster 3 mm Mortar 20 mm Concrete 120 mm Mortar 25 mm Tile 8 mm (inside)	Plaster 3 mm Mortar 20 mm Concrete 120 mm Styloform 25 mm Mortar 25 mm Tile 8 mm
Window Material	Glass 5 mm No Blind	Glass 5mm + 5mm Blind *1
Window Area divided by Total Surface Area	50 %	25 %
Air Distribution System	Low Efficient	High Efficient
Sensor Location for Fan-coil Unit	Side of Outlet	Front center of Fan-coil Unit
Interior Air Change Rate	10 [times/h]	4 [times/h]
Type of Interior Air Outlet	Grille mounted at High Sidewall	Anemostat Diffuser mounted on Ceiling

*1 If solar radiative gain is 349 W/m² or more than it, blinds of 80% are supposed to be shut. Even if solar radiative gain is than 349 W/m², blinds of 20% are supposed to be leaved close.

maximum heat supply requirements throughout the year, so that both the heat loads and *ML* could be offset.

While the above-mentioned factors were set at common levels throughout the simulations, two types of air distribution systems were examined—one inefficient from the viewpoint of preventing *ML* and the other efficient. These specifications are also described in Table 2. These elements were chosen based on the estimation models.

Operation

The time schedule for HVAC operation was as follows: preheating began at 0800, occupancy began at 0900, and operation ceased at 1800 from Monday to Saturday excluding Japanese national holidays. The nominal lighting load was preset at 20 W/m^2 and the nominal human load was preset at 10 W/m^2 as the sensible heat; these were varied according to the standard schedules preset in the program (Matsuo et al. 1980).

When panel heaters were used along with fan-coil units, they were principally assumed to be controlled to maintain the constant surface temperature of 50°C so that the total heater output was constant and the remaining heating load and *ML*/profit were offset by fan-coil units. When perimeter-zone cooling was required, the panel heaters were turned off, and only the fan-coil units were used to cancel the load. When the total heater output exceeded the perimeter-zone heating load with the surface temperature of the panel heater at 50°C, the fan-coil units were turned off, and the surface temperature of the panel heater was controlled to correspond to the sum of the heating load and the mixing energy loss/profit.

The factor that had much more influence on the *MLR* is the setpoint air temperature differential between the perimeter zone and interior zone. The outside air schedule was considered to be a reference in determining the perimeter setpoint air temperature. This means that the setpoint air temperature was changed according to the outside air temperature, as indicated in Figure 5. The temperature was raised as the outside air temperature fell below 10°C. This was done, for the thermal comfort of occupants in the perimeter zone, by compensating for cold radiation and/or the cold draft caused by the cooled outside wall.

Calculation, Method, and Conditions

Table 3 shows simulation conditions discussed in this study. Seven cases are discussed according to the combination of four elements: the outside wall insulation, the air distribution system, the presence of a panel heater, and the setpoint air temperature differential. In Case 7, the perimeter-zone air temperature is set at 18°C, which is 2°C lower than the interior zone. This is due to the influence of radiant heating.

The simulation took place for 152 days from November to March. Standard year climatic data for Tokyo were used

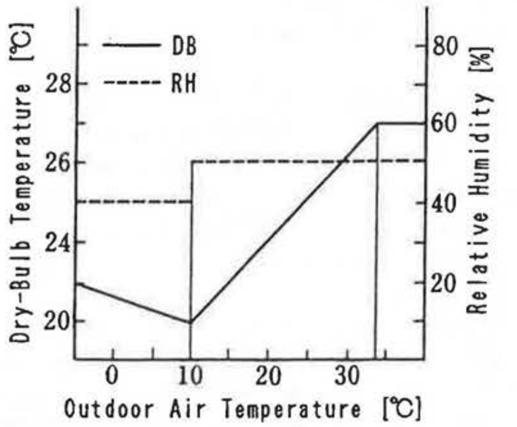

Figure 5 *Outdoor air temperature schedule for setting perimeter air temperature.*

for the weather conditions. These were statistically rearranged based on data from 10 years (1970-1979), which were recorded at the meteorological observatory (Matsuo et al. 1980).

For evaluation purposes, the total amounts of the ML as well as the actual heat supply for five months were used. The actual heat supply is defined as the sum of the base heat load and the total *ML*. Base heat load is the sum of the perimeter-zone heat load and the interior-zone heat load when the two zones are separated. This will be referred to as the ideal case. Here, as described in Part 1, only sensible heat was evaluated; latent heat was not considered.

An overall flow chart of the simulation is shown in Figure 6. The room heat loads, which are the bases for predicting the *ML*, are calculated using a computer code (Matsuo et al. 1980). This computer code can calculate the room heat load and room temperature/humidity trends every hour, to which the response factor method is applied to calculate the amount of heat transfer through the multilayered walls. The original program was improved by the authors, making it possible to determine the capacity of the apparatus at full-capacity operation during preheating and to calculate the temperature of the perimeter and interior zones with the assumption of partially or fully synthesizing both zones (Nakahara et al. 1988).

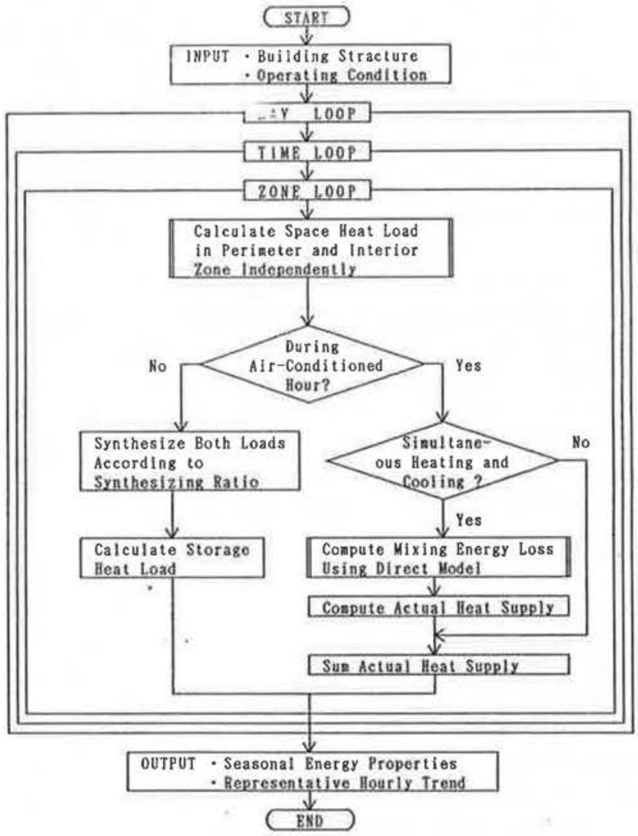

Figure 6 *Overall simulation flow chart.*

During operation, the perimeter-zone heat load and the interior-zone heat load were calculated every hour on the premise that these zones are independent of each other. The *MLs* are estimated using those values based on the direct estimation model of the *MLR*. When both the perimeter zone and the interior zone required either cooling or heating, there was no *ML*. As mentioned in Part 1, the *ML* cannot exceed twice as much as the lower amount of the perimeter-zone heating load or the interior-zone cooling load. When the predicted *ML* exceeded the maximum value, the *ML* was limited with it.

During non-operation, a clear boundary between the perimeter zone and interior zone vanished, but the two

TABLE 3
Simulation Conditions

Case	Outside Wall Insulation	Air Distribution System	Panel Heater	Set-point Temperature	
1	Low Insulation	High Efficiency	Not Use	P: 20	I: 20[℃]
2	Low	High	Not Use	P: 22	I: 20
3	High	High	Not Use	P: 20	I: 20
4	Low	Low	Not Use	P: 20	I: 20
5	High	Low	Not Use	P: 20	I: 20
6	Low	High	Not Use	P: Schedule	I: 20
7	Low	High	Use	P: 18	I: 20

*1 P : primeter zone, I : Interior zone
*2 Schedule means the outdoor air temperature schedule. Physical details are shown in Figure 5.

zones could not be regarded as completely uniform. Therefore, 50% of synthesizing was assumed to simulate the actual situation. That is, the natural temperature variation of each zone depends half on the thermal characteristics of the zone being considered and half on the synthesized thermal characteristics of both zones. If these two zones were not synchronized, the perimeter-zone heating load and the interior-zone cooling load might have been overestimated immediately after the start of the operation because the cooling effect for the interior structure could not appear in the calculation. As a result, the estimate of the seasonal mixing loss might have been excessive. Conversely, if the loads were completely synchronized, the seasonal mixing loss might have been underestimated. The computed results of these two extreme assumptions were also compared with the results of synthesizing 50% of the loads of the representative case.

RESULTS

The total amount of base heat load, the ML calculated with the regression equation, and the resulting heat supply requirements were obtained for every area in every zone and total area, as shown in Table 4 for all cases. For example, in the north zone in case 1, if the perimeter and interior zones are independent, a heating demand of 35.9 kWh/m^2 and a cooling demand of 14.0 kWh/m^2 occur over five months; therefore, a total demand of 49.9 kWh/m^2 is needed. However, because these zones are not actually independent, a mixing energy profit of 6.1 kWh/m^2 results, and a total supply heat of 43.8 kWh/m^2 is required, which is approximately 12% less than the base value. On the other hand, in case 2, a high *ML* of 20.4 kWh/m^2 results, so the total heat supply requirement amounts to 81.5 kWh/m^2, which is approximately 63% more than the ideal case.

The hourly trends of the base heat load and the *ML* produced in a representative week in case 1 are shown in Figures 7 and 8 for two zone areas. The hourly trends in the north area in a representative case are compared in Figures 9 through 11.

Hourly Trends

In every case, for two hours after the start of operation, no mixing energy loss/profit was produced, since heating was frequently required in both the perimeter zone and the interior zone due to a large storage heat load caused by intermittent operation. After that, as heating was replaced by cooling in the interior zone, simultaneous heating and cooling began.

In the south zone, the heating is usually applied in the morning and evening, but the cooling is often required on clear days for about three or four hours in the afternoon due to solar radiation. Therefore, the potential for *ML* in the south zone decreases compared with other zones. This situation sometimes appeared in the morning in the east zone or in the afternoon in the west zone; the north zone had the largest potential of *ML* of the four zones.

Influence of Setpoint Temperature Differential

Comparing case 1 with case 2, in which the perimeter- and interior-zone air temperatures were set equally, it is understood that the heat requirement dropped to approximately 62% of the case in which the perimeter-zone air temperature was set 2°C higher than in the interior zone. This occurred because both the base heating load and the *ML* decreased.

Comparing case 1 with case 6, when the outdoor air schedule was applied to set the perimeter-zone air temperature, the seasonal heating load was larger than when a 20°C fixed setting was used. This was because the perimeter-zone air temperatures were usually higher than 20°C, as the outdoor air temperatures were lower than 10°C. As a result, an *ML*, rather than a mixing energy profit, was obtained for the seasonal total amount.

In case 7, when panel heaters and fan-coil units were used for perimeter-zone heating in, the setpoint air temperature of the perimeter zone could have been set lower than that of the interior zone, under the constraint of thermal comfort. Therefore, it was assumed that this case, in which the panel surface temperature was 50°C, could be set 2°C lower than when panel heaters were not used. This case yielded a slightly larger mixing energy profit than case 1, in which equal setpoint temperatures were applied and panel heaters were not used, so that the seasonal heat requirement was reduced to approximately 84%. Since coexistence of the panel heaters must be evaluated from the viewpoint of not only reducing the seasonal energy requirement, but also improving the thermal environment in the perimeter zone, this method is suggested to be very worthwhile, as described in Part 1.

Influence of Other Variables

Outside Wall Insulation Comparing case 1 with case 3, upgrading the insulation of the outside wall prominently lessened the base heating load in the perimeter zone but slightly raised the base cooling load. As a result, though the mixing energy profit obtained was almost the same, the heat supply requirement was reduced by approximately 33% because of the drastic decrease in the base heating load.

Efficiency of the Air Distribution System From the viewpoint of preventing *ML*, efficiency resulted in a large difference from the seasonal *ML*. When air temperatures in the perimeter zone and interior zone were set equally, the efficient system, which would decrease the *ML*, resulted in mixing heat "profit" (cases 1 and 3), but the inefficient system resulted in "loss" (cases 4 and 5). Accordingly, the actual seasonal heat supply was reduced to about 74% with low insulation for the outside wall and about 84% with high insulation due to inefficient air distribution.

TABLE 4
Simulation Results

Case		Zone North	South	East	West	Total	
1	Base Heating Load	35.9	9.0	26.8	33.8	24.6	kWh/m²
	Base Cooling Load	14.0	35.5	13.9	14.4	21.9	
	Base Space Load	49.9	44.5	40.7	48.2	46.3	
	Mixing Energy Loss	-6.1	-1.9	-4.2	-4.6	-4.1	
	Actual Heat Supply	43.8	42.6	36.5	43.6	42.2	
2	Base Heating Load	46.0	14.3	37.3	44.5	33.1	
	Base Cooling Load	15.1	31.6	13.5	14.2	20.8	
	Base Space Load	61.1	45.9	50.8	58.7	53.9	
	Mixing Energy Loss	20.4	8.3	16.1	17.6	15.0	
	Actual Heat Supply	81.5	54.2	66.9	76.3	68.9	
3	Base Heating Load	2.6	0.4	1.1	1.7	1.5	
	Base Cooling Load	25.8	29.4	23.5	23.3	26.5	
	Base Space Load	28.4	29.8	24.6	25.0	28.0	
	Mixing Energy Loss	-1.8	-0.3	-1.4	-1.8	-1.2	
	Actual Heat Supply	26.6	29.5	23.2	23.2	26.8	
4	Base Heating Load	35.9	9.0	26.8	33.8	24.6	
	Base Cooling Load	14.0	35.5	13.9	14.4	21.9	
	Base Space Load	49.9	44.5	40.7	48.2	46.3	
	Mixing Energy Loss	15.8	5.0	11.6	12.8	10.9	
	Actual Heat Supply	65.7	49.5	52.3	61.0	57.2	
5	Base Heating Load	2.6	0.4	1.1	1.7	1.5	
	Base Cooling Load	25.8	29.4	23.5	23.3	26.5	
	Base Space Load	28.4	29.8	24.6	25.0	28.0	
	Mixing Energy Loss	5.5	0.9	5.0	5.6	3.8	
	Actual Heat Supply	33.9	30.7	29.6	30.6	31.8	
6	Base Heating Load	39.7	10.7	30.2	37.2	27.5	
	Base Cooling Load	14.4	33.6	13.3	13.6	21.1	
	Base Space Load	54.1	44.3	43.5	50.8	49.6	
	Mixing Energy Loss	2.3	0.8	1.6	1.4	1.5	
	Actual Heat Supply	56.4	45.1	45.1	52.2	51.1	
7	Base Heating Load	26.2	5.2	17.5	24.0	17.1	
	Base Cooling Load	13.4	40.8	15.5	15.4	23.9	
	Base Space Load	39.6	46.0	33.0	39.4	41.0	
	Mixing Energy Loss	-10.7	-1.6	-4.0	-5.2	-5.7	
	Actual Heat Supply	28.9	44.4	29.0	34.2	35.3	

Note

*1 Base heating/cooling loads mean that those when the perimeter zone and the interior zone are separated independently, in other words, when the mixing energy loss and/or the mixing energy profit are not generated at all. They are summed without classification for the perimeter zone or the interior zone. Base space load shows sum of the base heating load and the base cooling load.

*2 These all values means total amount of heat for 152 days from November to March.

*3 Floor areas of north, south, east and west zone are 576, 576, 216 and 216 m²; Total floor area is 1584 m². These values are used as denominators for presentation of total amounts of heats.

Influence of Load Synchronizing During Non-Operation

The computed results for the three different synchronizing ratios during non-operation—not synchronized, 50% synchronized, or completely synchronized—are compared in Table 5. Hourly trend examples for these cases are compared in Figure 12.

When a synchronizing ratio of 0% is assumed, cooling was generated in the interior zone at the start of system operation because the slab cooling effect due to natural convection could not be expected. When a ratio of 50% or 100% was applied, the interior zone required heating after a few hours following start of the operation due to the presence of stored heat in the slab. Furthermore, the cooling load required when the office was occupied was less than in the unsynchronized case. As a result, the increase in the synchronizing ratio decreased both the seasonal base heating and cooling loads in every direction so that the seasonal mixing energy profit was reduced. However, the seasonal heat requirement was lessened because of the drastic reduction of the base loads due to the mixing profit of the heat load. On the other hand, there was not a large difference in the seasonal cooling and heating loads when the synchronizing ratios were between 50% and 100%.

The actual synchronizing percentage differs, mainly due to the depth of the interior zone and the amount of furniture

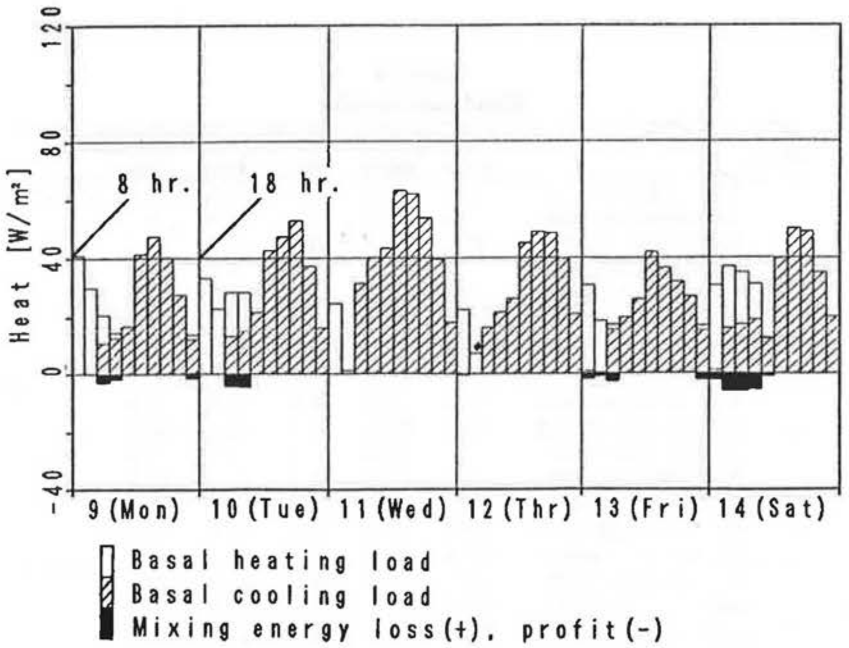

Figure 7 *Hourly trends of the basal heat loads and the mixing energy loss in representative week: Case 1, south.*

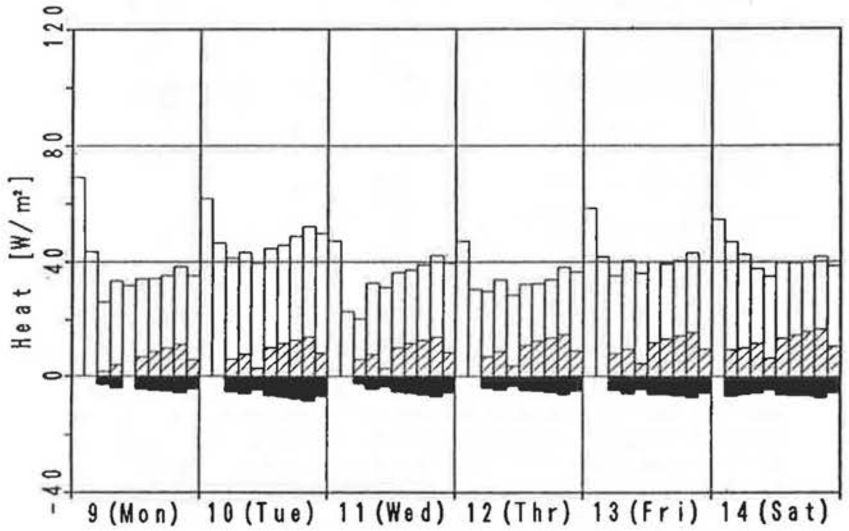

Figure 8 *Hourly trends of the basal heat loads and the mixing energy loss in representative week: Case 1, east.*

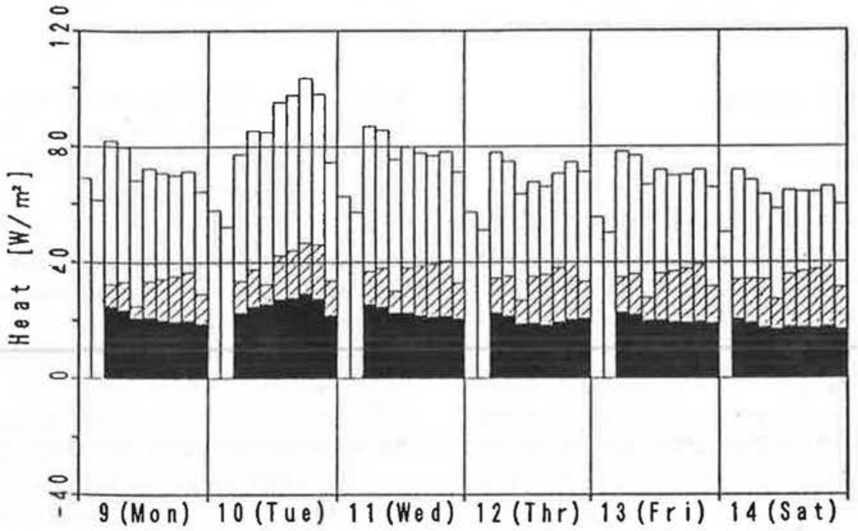

Figure 9 *Hourly trends of the basal heat loads and the mixing energy loss in representative week: Case 2, north.*

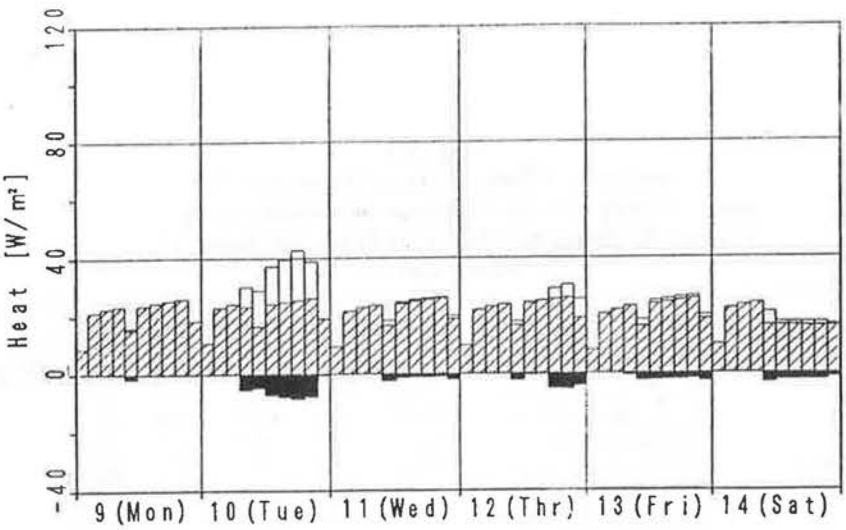

Figure 10 *Hourly trends of the basal heat loads and the mixing energy loss in representative week: Case 3, north.*

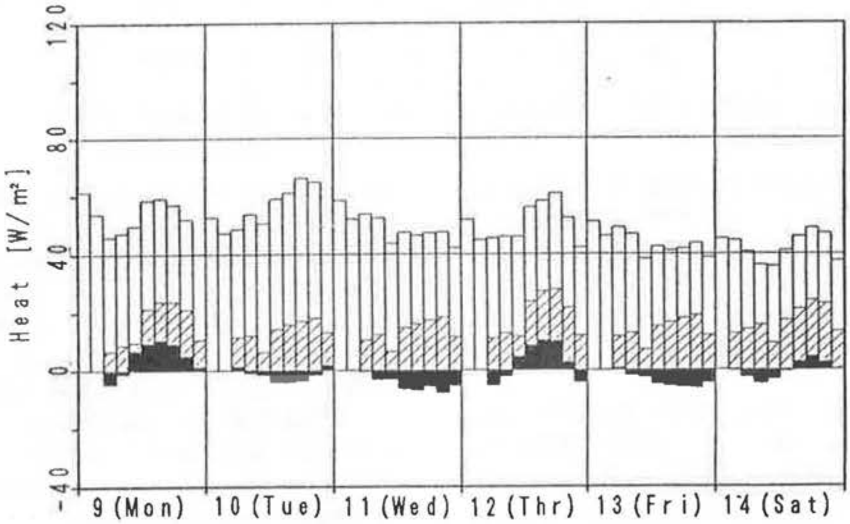

Figure 11 *Hourly trends of the basal heat loads and the mixing energy loss in representative week: Case 6, north.*

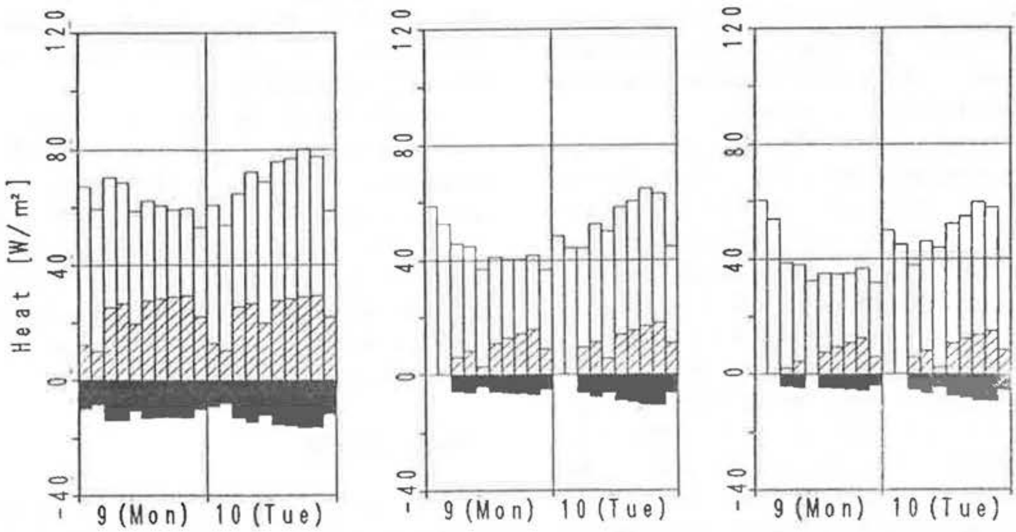

(a) 0% (b) 50% (c) 100%

Figure 12 *Comparison of hourly trends of the basal heat loads and the mixing energy loss in representative week among three different assumptions on synchronizing between the perimeter and interior heat load in off-operation: Case 1, north.*
(a) 0% of load synchronizing. (b) 50% of load synchronizing. (c) 100% of load synchronizing.

TABLE 5
Influence of Computational Assumption for Synchronizing between Perimeter and Interior Zone Heat Loads during Non-Operation Hours on Seasonal Heat Properties

Synthesizing Ratio	Case 1	Zone					
		North	South	East	West	Total	
	Basal Heating Load	39.9	10.6	29.7	36.8	27.4	kWh/m²
0 %	Basal Cooling Load	28.4	43.8	27.4	27.7	33.7	
	Basal Space Load	68.3	54.4	57.1	64.5	61.1	
Non-	Mixing Energy Loss	-11.0	-4.0	-9.9	-11.0	-9.0	
Synthesizing	Actual Heat Supply	57.3	50.4	47.2	53.5	52.1	
	Basal Heating Load	35.9	9.0	26.8	33.8	24.6	
50 %	Basal Cooling Load	14.0	35.5	13.9	14.4	21.9	
	Basal Space Load	49.9	44.5	40.7	48.2	46.3	
Half-	Mixing Energy Loss	-6.1	-1.9	-4.2	-4.6	-4.1	
Synthesizing	Actual Heat Supply	43.8	42.6	36.5	43.6	42.2	
	Basal Heating Load	33.8	8.6	25.0	32.0	23.1	
100 %	Basal Cooling Load	11.1	34.4	11.4	11.8	19.7	
	Basal Space Load	44.9	43.0	36.6	43.8	42.8	
Complete-	Mixing Energy Loss	-4.8	-1.5	-3.0	-3.3	-3.1	
Synthesizing	Actual Heat Supply	40.1	41.5	33.6	40.5	39.7	

in the room. This point is not discussed in detail in this paper, but the authors expect that a 50% synchronizing is reasonable.

DISCUSSION OF THE SIMULATION RESULTS FOR OPTIMUM DESIGN

Since the case studies were conducted for a typical office and for a standard climate, the results can be compared and discussed on the applicable general level.

As is expected for the regressive models, the influence of the setpoint air temperature differential between the perimeter and interior zones on the actual seasonal heat supply is very large. If the air temperature setting of the perimeter zone is 2°C higher than that of interior zone, an approximately 60% larger heat supply is required than with an equal setting. Such a setting must, therefore, be avoided from the viewpoint of energy conservation.

However, an equal setting of the perimeter-zone and interior-zone air temperatures cannot provide equal thermal comfort because of the strong draft and cold radiation from the outside walls. When the outdoor air schedule is applied to allow for perimeter-zone thermal comfort, the ML, though slight, is generated seasonally. Therefore, the heat supply requirement is 20% more than if the settings were equal. However, if the perimeter-zone air temperature is 2°C lower than the interior zone, which requires radiant heating to compensate for the different comfort levels in the perimeter and interior zones, the seasonal supply heat requirement is reduced to approximately 83%. It is, therefore, effective to lower the perimeter-zone setpoint temperature while applying radiant heating with fan-coil units to lessen the seasonal energy consumption under the constraint of thermal comfort.

When the perimeter-zone air temperature and the interior-zone air temperature are set equally, a mixing energy profit, though only approximately 8% of the base space load, can be obtained if the air distribution system is effective. However, an improperly designed system with a large interior air change rate yields a larger amount of *ML*—20% of the base space load. Efficient design of the air distribution system is, therefore, a very important factor for reducing seasonal energy consumption.

Upgrading the insulation of the outside walls can reduce the perimeter-zone heating load. On the other hand, decreasing the perimeter-zone heating load weakens the potential for mixing energy profit as well as for *ML*. From the viewpoint of reducing the energy requirement, the former improvement yields a larger effect on the decrease in the actual heat supply than the latter failure when a mixing profit is obtained. Therefore, insulating the outside wall and decreasing the window surface area are effective for energy conservation.

If a mixing energy "loss" is expected to be produced, when, for example, an inefficient air distribution system is designed, insulating the outside wall can provide synergistic energy-saving effects: a decrease in the base heating load and the *ML*. That is, an improvement of the air distribution system can yield much larger effects for a structure with low insulation than a structure with high insulation. In other words, a structure with low insulation should require a highly efficient air distribution system.

CONCLUSIONS

The concept of two models for estimating the *ML* in a simultaneously heated and cooled room was developed based on the experimental results described in Part 1. One was a direct estimation model in which the *ML* was directly and linearly related to many design/control factors. The other was the ventilation model, which was based on the deduction that a setpoint air temperature differential between the perimeter and interior zones had the greatest influence on the *ML*. In the latter, the equivalent flow coefficient of an ideal opening was the unique parameter to be identified. These models were identified using multiple regression analyses of data from 129 experiments. Both models had a high coefficient of correlations from a practical viewpoint, while the direct estimation model had a slightly higher coefficient value than the ventilation model, so the former was used for the discussion of seasonal energy evaluations.

Based on the improved dynamic heat-load calculation, quantitative evaluations of the seasonal properties of the ML and the actual heat supply requirement during winter were conducted under typical office and standard Tokyo climatic conditions. The effects of certain factors, such as outside wall insulation and air distribution system performance, were calculated and discussed.

The major conclusions were as follows:

1. The influence of the setpoint air temperature differential between the perimeter and interior zones on actual seasonal heat supply is very large. A 2°C higher setting of the perimeter-zone air temperature requires approximately 1.6 times the amount of heat supply compared to the case where the settings are equal.

2. When the outdoor air temperature schedule is applied to allow for perimeter-zone thermal comfort, the *ML*, though slight, is generated seasonally, so that the heat supply requirement is 1.2 times more than in the case where the settings are equal, when the perimeter-zone environment is poor.

3. A 2°C lower setting of the perimeter-zone air temperature, enabled by applying radiant heating to allow for thermal comfort in that zone, requires approximately half the seasonal heat supply of a 2°C higher setting without radiant heating.

4. Highly insulated outside walls can reduce the seasonal heat supply requirement by two-thirds when compared with poorly insulated outside walls because the perimeter heating load is drastically reduced, even though the obtained mixing energy profit is decreased.

5. An inefficient air distribution system, from the viewpoint of protecting the *ML*, requires about 1.3 times the seasonal heat supply as an efficient system. The energy-saving effect obtained by improving the efficiency of the distribution system is larger in a structure with low insulation than in a structure with high insulation.

6. Concerning the load computation assumption during hours of non-operation, when a synchronizing ratio of 0% is assumed between the perimeter-zone and interior-zone heat loads, both the base heat load and the *ML* generated and, also, the resultant actual heat supply requirement increased about 25% compared with a synchronizing ratio of 50% used as a basic ratio in the case studies mentioned above. On the other hand, a synchronizing ratio of 100% gave almost the same actual heat supply as the basic ratio.

ACKNOWLEDGMENTS

This study was conducted in part under a Grant-in-Aid for Scientific Research, Task No. 58420037, from the Japanese Ministry of Education, Science and Culture.

NOMENCLATURE

ML	=	mixing energy loss, W/m^2
MLR	=	mixing energy loss ratio
X_i	=	ith variable involved in a regressive equation
a_i	=	regressive coefficient of x_i in direct estimation model
a_o	=	regressive constant in direct estimation model
b_i	=	regressive coefficient of x_i in direct estimation model
b_o	=	regressive constant in direct estimation model
Q_{p-i}	=	air volume rate moving from perimeter to interior, m^3/h
Q_{i-p}	=	air volume rate moving from interior to perimeter, m^3/h
h_1	=	height between ceiling level and neutral level for pressure differential, m
h_2	=	height between floor level and neutral level for pressure differential, m
W	=	room width, m
g	=	gravity acceleration, m/s^2
y	=	height from neutral level, m
H	=	room height, m
c	=	specific heat of air, W·h/kg·K
t_p	=	setpoint air temperature in perimeter zone, °C

Greek Letters

α	=	equivalent flow coefficient of ideal opening
θ_p	=	representative temperature in perimeter zone, °C
θ_i	=	representative temperature in interior zone, °C
γ_p	=	air density at temperature of θ_p, kg/m^3
γ_i	=	air density at temperature of θ_i, kg/m^3
$\Delta\gamma$	=	$\gamma_p - \gamma_i$
$\Delta\theta$	=	$\theta_p - \theta_i$
Δt_p	=	supply air temperature differential in perimeter zone, °C
Δt_i	=	supply air temperature differential in interior zone, °C

REFERENCES

Ito, H., and N. Nakahara. 1987. Studies on prevention of mixing energy loss in air-conditioned room. Part 2, Estimation of seasonal energy loss. *Transactions of SHASE*, No. 33, pp. 13-22 (in Japanese).

Ito, H., and N. Nakahara. 1989. Studies on prevention of mixing energy loss in air-conditioned room. Part 3, Effects of type of interior air outlet and heat storage load on energy loss, and property of room air temperature distribution. *Transactions of SHASE,* No. 41, pp. 51-60 (in Japanese).

Matsuo, Y., K. Yokoyama, H. Ishino, and S. Kawamoto. 1980. *Guide to dynamic heat load calculation in HVAC system*. Japanese Association of Building Service Engineers (in Japanese).

Nakahara, N., and K. Sagara. 1988. Water thermal storage tank: Part 1—Basic design concept and storage estimation for multiconnected complete mixing tanks. *ASHRAE Transactions* 94(2).

Nakahara N., K. Shimada, and H. Yuzawa. 1988. Study on estimation procedures of heating, requirements at preheating period. *Transactions of SHASE*, No. 38, pp. 33-44 (in Japanese).